



HAL
open science

Far-field radiative thermal rectification with bulk materials

Sreyash Sarkar, Elyes Nefzaoui, Philippe Basset, Tarik Bourouina

► **To cite this version:**

Sreyash Sarkar, Elyes Nefzaoui, Philippe Basset, Tarik Bourouina. Far-field radiative thermal rectification with bulk materials. *Journal of Quantitative Spectroscopy and Radiative Transfer*, 2021, 266, pp.107573. 10.1016/j.jqsrt.2021.107573 . hal-03527225

HAL Id: hal-03527225

<https://hal.science/hal-03527225>

Submitted on 10 Mar 2023

HAL is a multi-disciplinary open access archive for the deposit and dissemination of scientific research documents, whether they are published or not. The documents may come from teaching and research institutions in France or abroad, or from public or private research centers.

L'archive ouverte pluridisciplinaire **HAL**, est destinée au dépôt et à la diffusion de documents scientifiques de niveau recherche, publiés ou non, émanant des établissements d'enseignement et de recherche français ou étrangers, des laboratoires publics ou privés.



Distributed under a Creative Commons Attribution - NonCommercial 4.0 International License

Far-field Radiative Thermal Rectification with Bulk Materials

Sreyash Sarkar*, Elyes Nefzaoui*, Philippe Basset, Tarik Bourouina

ESYCOM, Univ Gustave Eiffel, CNRS, CNAM, ESIEE Paris, F-77454 Marne-la-Vallée, France

Abstract

In this paper, we explore the far-field radiative thermal rectification potential of common materials such as metals, ceramics and doped semi-conductors using radiative and thermo-radiative properties extracted from literature. Seventeen different materials are considered. The rectification coefficient is then calculated for 136 pairs of materials; each pair can be used for the two terminals of a radiative thermal diode. A thermal bias of 200 K is considered. The choice of materials and thermal bias value are only bound by data availability in literature. Obtained results, highlight new candidate materials for far-field radiative thermal rectification. They also highlight materials where thermal rectification is not negligible and should be considered with care in heat transfer calculations when considering systems subject to a comparable thermal bias and where these materials are used. Among the materials studied, undoped Indium Arsenide (InAs) shows great promise to be employed for thermal rectification, with a thermal rectification ratio reaching 96.35% in combination with other materials. Obtained results pave the way for an optimized design of thermal radiation control and management devices such as thermal diodes.

Keywords: radiative thermal rectification, bulk materials, far-field

*Corresponding author
Email addresses: sreyash.sarkar@esiee.fr (Sreyash Sarkar),
elyes.nefzaoui@esiee.fr (Elyes Nefzaoui)

1. Introduction

Thermal rectification (TR) can be defined as an asymmetry in the heat flux when the temperature difference between two interacting thermal reservoirs is reversed. Therefore, a two-terminal thermal device exhibits thermal rectification if it transports heat in one direction with more ease than in the reverse direction. Thermal rectification has been a subject of intrigue since its underlying test perception in 1936 by Starr [1] because of its aptitude to open up innovation in heat transport control, inspiring analogies to the tremendous advancement in the electronics industry following the invention of such nonlinear elements as the transistor and the diode. Other potential applications of thermal rectification include thermal barrier coatings [2], enhanced efficiency thermo-electric devices [3, 4], temperature variation driven heat engines[5] and radiative cooling[6, 7]. From that point forward, several investigations have been performed to understand which systems can exhibit thermal rectification[8] and have introduced the concepts of numerous innovative devices like thermal transistors [9, 10, 11, 12], thermal logic circuits[13, 14, 15, 16, 17] and thermal diodes[18, 19, 20, 21, 22, 23]. Recent investigations of thermal rectification have covered different heat transfer(HT) modes including conduction [24, 25], convection [26] and radiation [27, 28, 29, 30, 31, 32, 33, 34]. We describe the main current trends in the following paragraphs and more extensive reviews can be found in [8, 35].

To achieve conductive thermal rectification, several mechanisms have been proposed including thermal potential barrier between material contacts[27], thermal strain/warping at interfaces of two materials[28], nanostructured geometric asymmetry[36] and anharmonic lattices[31]. The asymmetry at the interface between two materials due to the difference of their thermal conductivity temperature dependence has also been shown to be the main driving mechanism for conductive thermal rectification by

Marucha et. al[37] and subsequently used in the models of Hoff et. al[38], Sun et. al[39] and in Go et. al[40]. Based on the same principle, Hu et al[41] and Zhang et. al[24] presented thermal rectifiers based on different thermal conductivities of dissimilar graphene nano-ribbons or Y junctions. At the micro and nano-scales, the asymmetry at the origin of TR can be widely tuned and engineered in nano-structured materials [42] which led to many contributions using several phenomena observed in a large diversity of nano-structures such as ballistic phonons anisotropy at large thermal bias [2], phonons lateral confinement[43] and the temperature dependence of lattice vibrations density of states[44]. Solid-state thermal rectifiers have also been proposed taking benefit of nonlinear atomic vibrations[31][45], nonlinear dispersion relations of the electron gas in metals[46], and thermal streams through Josephson junctions[47] or metal-superconductor nano-intersections[48]. At even smaller scales, TR in quantum systems has recently lured researchers such as in the work of Landi et.al[49] on TR using a quantum XXZ chain subject to an inhomogeneous field and the research of Chi et. al [49] discussing TR in a system of a single level quantum-dot connected to ferromagnetic leads. On the other hand, Scheibner et al[50] experimentally demonstrated a TR behavior in quantum dots subject to high in-plane magnetic fields[50] and most recently in the work of Senior et. al[51], it has been shown that a superconducting quantum bit coupled to two superconducting resonators can achieve magnetic flux-tunable photonic heat rectification between 0 and 10%.

Radiative heat transfer is another heat transfer mode that has been actively investigated for thermal rectification application in the past decade after the seminal works of Ruokola et. al[52] and Otey [32]. Two main paths have been considered. On one hand, near field (NF) Radiative Thermal Rectification (RTR) between materials supporting resonating surface waves separated by wavelength scale or sub-wavelength gaps. Plasmonic materials supporting surface plasmon polaritons and dielectrics supporting surface phonon polaritons have been mainly considered. Used materials for NF RTR include

gold and silicon [53, 54] with temperatures between $300K$ and $600K$, doped silicon[55], SiC [32, 33, 56], SiC and SiO₂ [57, 34] , InSb and graphene-coated SiO₂[58]. Many works on NF RTR also used phase change materials and mainly Vanadium Dioxide (VO_2)[59, 60, 61, 62], and more rarely, thermochromic materials [63]. In addition to the diversity of used materials, a large variety of geometries and sizes has been explored as in the work of Shen et. al[36], which elucidated non-contact thermal diodes using asymmetric nanostructures while [64, 65] reported on Near field RTR in the deep sub-wavelength regime between planar surfaces separated by nanometre-scale distances. Zhou et. al[66] proposed for instance a thermal diode using a nanoporous plate and a plate, both made of silicon carbide and where the two terminals are separated by a nanometric vacuum gap while Ott et. al[21] explored a radiative thermal diode made of two nanoparticles coupled with the nonreciprocal surface modes of a magneto-optical substrate.

On the other hand, far-field (FF) radiative heat transfer also enables RTR and has been an active area of interest in the past decade. Compared to NF RTR, FF RTR provides the advantage of simplicity and ease of fabrication since it does not require the combination and alignment of objects separated by micro-metric or nano-metric gaps. Two main solutions have been reported for this purpose : the use of phase change materials (PCM) [11, 67, 20] and tunable metamaterials often used as selective radiation emitters and absorbers[68]. The use of phase change materials, and VO_2 in particular, is predominant in both conceptual [69] and experimental works [70, 71]. Recently, Ghanekar et. al[72] proposed the concept of a far-field radiative thermal rectifier combining both PCM, VO_2 for instance, and a Fabry-Perot cavity based meta-material. Beyond thermal rectification, various radiative heat transfer control devices have been proposed such as thermal transistors [73, 9, 10, 11, 12] and photonic thermal memristors [74] . The large majority of those PCM based far-field radiation control devices use VO_2 since the seminal work of Van Zwol et. al[75] who provided a comprehensive characterization of VO_2 radiative and

thermo-radiative properties (TRP) around its metal-insulator transition temperature. Surprisingly, the good performances of VO_2 for RTR seem to have prevented authors from exploring other materials, contrarily to the what have been done and reported for NF RTR. Indeed, the large variety of existing materials have not been systematically considered to assess their potential use in FF RTR. This can be legitimately explained by the scarcity of literature on materials' radiative properties in the wavelength range of interest for thermal radiation and their subsequent temperature dependence. However, a thorough investigation of commonly available materials performances with respect to thermal rectification has not been realized up until now.

In the present work, we present an evaluation of RTR potential of different materials commonly used in micro-fabricated devices such as Indium Arsenide, Gallium Arsenide, Gallium Antimonide, Germanium, Zinc Sulphide, Silicon, metals such as Platinum, Copper, Nickel, Gold, refractory metal such as Tungsten and ceramics like Titanium Nitride, Ruby, Corundum and rare-earth material such as Neodymium Gallate, based on radiative and thermo-radiative properties available in literature. The paper is organized as follows: in the present section, we introduce the concept of thermal rectification along with a brief review of the works accomplished so far and delineate the pertinence of the present work; next in section 2, we explain the principle of radiative thermal rectification and introduce the main quantities that govern and characterize a radiative thermal rectification behavior. We also, describe the used radiative and thermo-radiative properties of the considered materials and the process of relevant data extraction from literature. Finally, we report and discuss the main results on the radiative thermal rectification potential of the considered materials in section 3.

2. Method

2.1. Theory

Variation of the heat flux magnitude when the sign of the temperature gradient between two points is reversed is the basic definition of thermal rectification. Let us consider two thermal reservoirs 1 and 2 at two different temperature T_1 and T_2 , respectively, with $T_2 > T_1$. The temperature difference between the two reservoirs is noted $\Delta T = T_2 - T_1$. This temperature difference results in heat flux Φ_F . We will refer to this initial configuration as forward bias configuration. If we invert the temperature difference between the two reservoirs, i.e if we set reservoir 1 temperature to T_2 and reservoir 2 temperature to T_1 , a reverse bias flux Φ_R is observed. Thermal rectification occurs when the heat fluxes in forward Φ_F and reverse bias Φ_R , under the same magnitude of the thermal potential difference, i.e for a constant $|\Delta T|$ but with opposite ΔT signs, are unequal. Thermal rectification is generally quantified, even though it is not the only indicator encountered in the literature, by means of the normalized rectification coefficient [1, 8] which can be defined as:

$$R = \frac{|\Phi_F - \Phi_R|}{\max(\Phi_F, \Phi_R)} \quad (1)$$

where, Φ_F and Φ_R denote the heat flux under forward and backward bias, respectively. In this paper, the definition of normalized rectification coefficient given in equation 1 is preferred because it provides bound rectification coefficient values between zero and one, as opposed to alternative definitions adopted by some authors[76, 48] which lead to values from zero to infinity. A schematic of two thermal reservoirs exchanging heat flux in forward and reverse bias configurations is given in 1.

In this paper, we consider the simple case of far-field radiative thermal rectification between two semi-infinite planes, separated by a vacuum gap of thickness d , characterized by their radiative optical properties (their temperature dependent emissivities and reflectivities). Therefore, the distance separating the two planes exchanging heat by radiation is much larger than

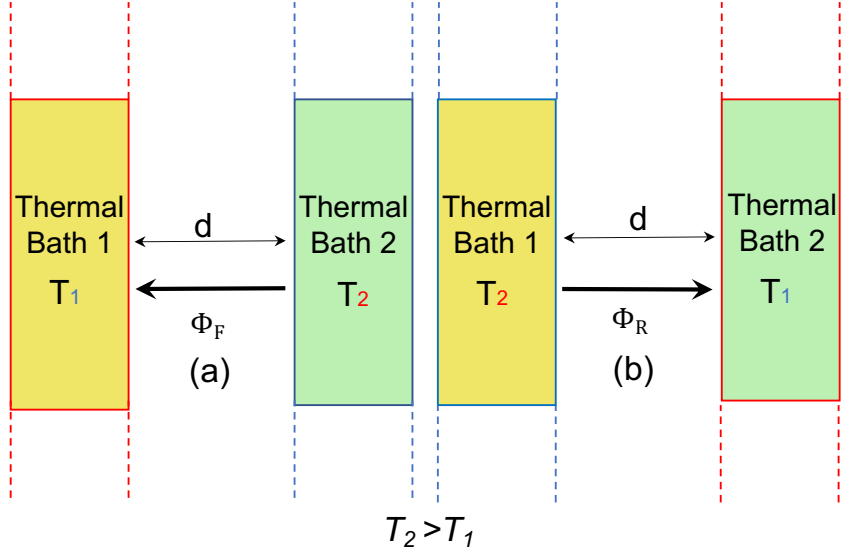


Figure 1: (a) Forward and (b) Reverse bias conditions of HT between two semi-infinite planes acting as thermal baths separated by a vacuum gap of thickness, d . Thermal rectification occurs only when, Φ_F and Φ_R denoting the heat flux in the forward and reverse operating modes under two temperatures ($T_2 > T_1$), are unequal. The gap width (d) is assumed to be much larger than the dominant thermal radiation wavelength (Wien wavelength, $\lambda_W(T)$).

the characteristic wavelength of thermal radiation at the considered bodies temperatures given by Wien's law : $d > \lambda_W(T)$, where $\lambda_W(T) = \frac{hc^2}{5k_B T}$, where h , c , k_B and T are Planck's constant, the speed of light in vacuum, Boltzmann constant and the absolute temperature respectively. For simplicity's sake, we also assume they are both Lambertian sources, meaning that their emissivities and reflectivities ($\epsilon(\lambda, T)$ and $\rho(\lambda, T)$ respectively) are direction independent[77]. Considering these assumptions, the net radiative heat flux (RHF) exchanged by the two bodies resumes then to the far field contribution, which can be written as[57]:

$$\Phi(T_1, T_2) = \pi \int_{\lambda=0}^{\infty} [I^0(\lambda, T_1)I^0(\lambda, T_2)]\tau(\lambda, T_1, T_2)d\lambda \quad (2)$$

where,

$$I^0(\lambda, T) = \frac{hc^2}{\lambda^5} \frac{1}{e^{\frac{hc}{k_B T}} - 1} \quad (3)$$

is the black body intensity at a temperature T and wavelength λ , where h , c , k_B and T are Planck's constant, the speed of light in vacuum, Boltzmann constant and the absolute temperature respectively[78] and

$$\tau(\lambda, T_1, T_2) = \frac{\epsilon(\lambda, T_1)\epsilon(\lambda, T_2)}{1 - \rho(\lambda, T_1)\rho(\lambda, T_2)} \quad (4)$$

is the monochromatic RHF density transmission coefficient between 1 and 2, where $\epsilon(\lambda, T)$ and $\rho(\lambda, T)$ is the monochromatic emissivity and reflectivity at a given temperature respectively. The RHF density transmission coefficient is governed by the radiative properties of the two considered thermal baths, in particular their emissivities and reflectivities and the temperature dependence of these properties. These properties are completely governed by the considered bodies dielectric functions and geometries. In the case of opaque bodies, energy conservation[77] and Kirchhoff's laws [77] combination leads to the following relation between the monochromatic emissivity, reflectivity and transmittivity at a given temperature:

$$\epsilon(\lambda, T) = 1 - \rho(\lambda, T) - t(\lambda, T) \quad (5)$$

Therefore, to evaluate the thermal rectification potential of a given pair of materials, we need to know the emissivity, reflectivity and transmittivity of each terminal of the considered thermal diode and its temperature dependence. Since the emissivity and reflectivity depend on the dielectric function, knowing the dielectric permittivity or the complex refractive index of the considered materials is also sufficient to estimate their potential for thermal rectification. In our case, these data have been harvested from literature.

2.2. Radiative properties data extraction

Thermo-radiative properties, i.e materials radiative properties and their temperature dependence, are the main input data required to assess the radiative thermal rectification ability of a given material. Difficulty to obtain such data, especially in the wavelength range of thermal radiation from room temperature to a few hundred Kelvins above room temperature,

i.e. in the mid and far-infrared, perhaps explains the dearth of literature on thermal rectification with the large variety of existing materials and the strong concentration of literature on VO_2 . Although the most important material libraries in this regard such as The Handbook of Optical Materials by Edward D. Palik [79] and that of Weber[80], provide an exhaustive collection of material optical properties, unfortunately, available data is not temperature dependent. Radiative properties of common materials at different temperatures, in the required infrared range, are scantily available in literature. Incidentally, the majority of relevant data found, regarding the works dedicated to this sub-area of research, are pertaining to the study of semiconductors. The optical properties of metals such as, Gold [81, 82], Aluminum [83, 84], Tungsten [82], Molybdenum[85], Silver [86], Copper [87], Nickel [87] have been studied, but unfortunately researchers have not been particularly interested in exploring the aforesaid optical properties at higher temperatures and at larger wavelengths, adherent to the IR range, which is an imperative in this study. Materials like Si [33] and Ge [88] have been considered broadly, beginning in the 1950's. GaAs, InAs, InP, and GaSb make a case for volumes of research of their own and have been utilized as a part of light emanating and optoelectronic devices [89]. Material properties were learned at temperatures extending from low temperatures (liquid helium, 4.2 K, or liquid nitrogen, 77 K) to about room temperature, 298 K [89]. The 2010 work of Thomas R. Harris [89] provides valuable experimental data on the study of optical properties of Germanium, Gallium and Indium derivatives and on Bulk Silicon, at various temperatures. Optical properties of Silicon Carbide [90, 91], and on Zinc Sulphide [92] have also been reported in the past decades. The use of numerical simulation data for bulk silicon generated using a Drude Model was also suggested in [93, 94], and we took use of this model to produce temperature dependent radiative properties data for bulk silicon. The list of materials considered in the present study is indicated in Table .2.

In the work of Thomas R. Harris[89], temperature dependent

Table 1: Considered Materials

Materials	Symbols
Semiconductors	
Germanium[89, 95]	Ge
Gallium Derivatives[89, 96]	GaAs,GaSb
Undoped Indium Arsenide[89, 97, 98]	InAs
Zinc Sulphide [92, 99, 100, 101]	ZnS
Silicon Carbide[57, 90]	SiC
Bulk Doped N-type Silicon($1 \times 10^{20} \text{cm}^{-3}$)	DBuSi ₁
Bulk Doped N-type Silicon($3 \times 10^{20} \text{cm}^{-3}$)	DBuSi ₃
Metals	
Gold [81, 82]	Au
Copper[87]	Cu
Platinum[102]	Pt
Nickel[103]	Ni
Tungsten[104]	W
Ceramic Materials	
Titanium Nitride[105]	TiN
Corundum[106]	Al_2O_3
Ruby[107]	$Al_2O_3 : Cr$
Rare Earth Materials	
Neodymium Gallate[107]	$NdGaO_3$

transmission measurements for Ge were taken up to approximately 650 K. The data was taken in near IR and mid IR wavelength ranges. Comparison with older literature[108] shows good agreement, indicating that the measured data are reliable. Similarly, temperature dependent transmission measurements were taken up to approximately 850 K for undoped GaAs and up to approximately 550 K for n-type GaAs doped with silicon. In the case for undoped GaSb, measurements were taken up to 650 K. Unfortunately, for sulphur doped

InP, only near IR measurements were reported, which renders the data set incomplete for usage in the present study[89]. Thus, temperature dependent

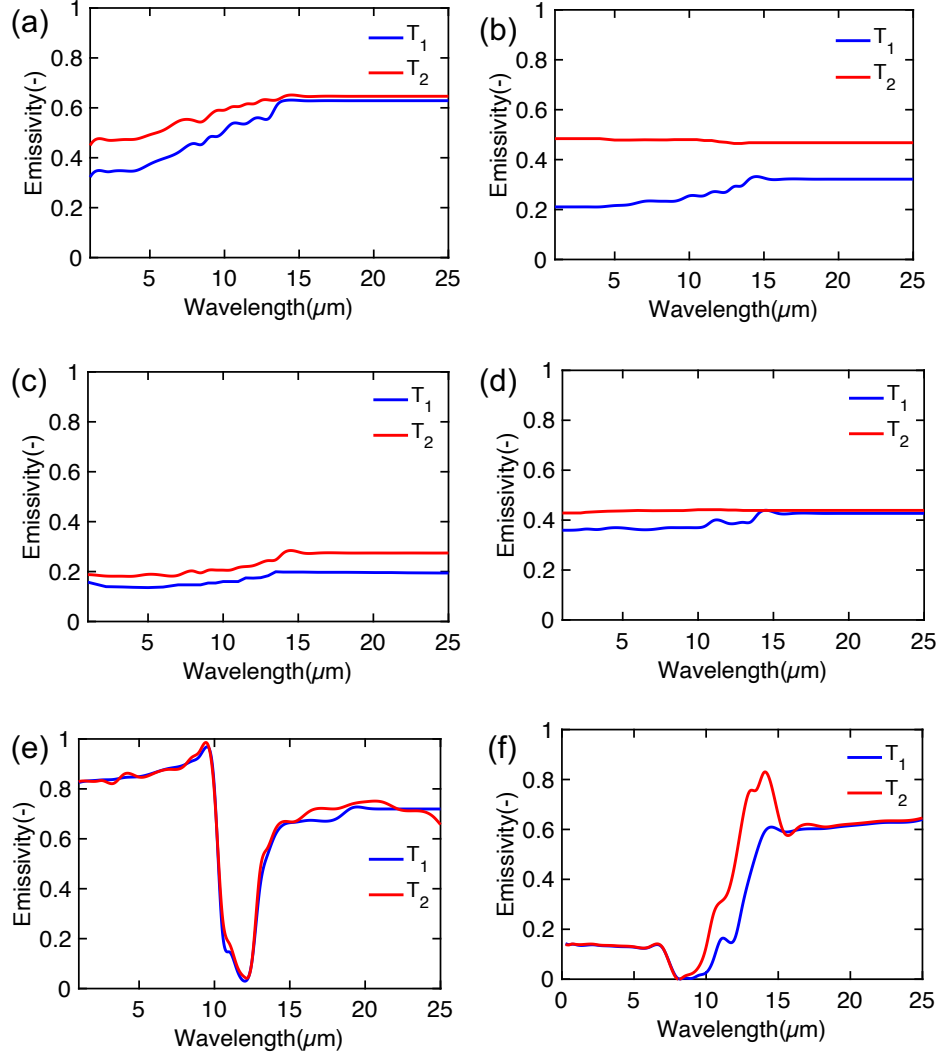


Figure 2: Emissivity of a few common materials found in literature-(a) GaSb (b) InAs (c) GaAs (d) Ge (e) SiC (f) ZnS at $T_1=300\text{K}$ and $T_2=500\text{K}$.

transmission measurements were carried out for Si, Ge, GaAs, GaSb, InAs, and InP from 0.6 to 25 μm at temperatures ranging from 295 up to 900 K. Band gap shifts were observed as temperature changed and were compared to

previous works. General agreement was observed in the trend of the change in the band gap with temperature, however, the actual band gap energy values deviated from the expected-on average by about 10 %. The reflectivity maximum increased in magnitude with increasing temperature, with successful measurements being done up to 517 K[89].

To completely gather temperature dependent reflectivity data of GaAs, GaSb, InAs, Ge another set of works were adhered to such as the work of Skauli et. al[96], where the refractive index of GaAs has been measured. From 1979-1984, H. H Li[95, 99] prepared a comprehensive report on the temperature dependence of the refractive indices of Si, Ge, ZnS, ZnSe, ZnTe etc., where he provided near non-existent temperature-dependent data on these particular semi-conductors refractive index in a wide spectral range including mid and far infra-red.

For SiC in the IR wavelength range from 1 μm to 25 μm , many data are available in literature and because much of SiC optical properties depend on its crystallographic orientation [109, 110], they have been compared to other semiconductor relevant data with care. Some widely cited sources are that of Bohren et. al [111], Mutschke et al.[112, 113], the measurements of Daniel Ng [90] and Joulain et. al [57]. Cagran et. al[114] provided a comprehensive study on the temperature-resolved infrared spectral emissivity of SiC and this data was finally employed in the present study due to its reportage of wide and flexible temperature dependence of emissivity.

On the other hand, the measurements on Zinc Sulphide (ZnS) reported in [92, 100, 101] provide valuable insight into the thermal, structural and optical properties of a commercially available sample of multispectral ZnS. The hemispherical transmission, reflectivity, absorptivity, emissivity of unpolarized light at normal incidence on ZnS at 24 °C, 100 °C and 200 °C are reported in [92].

While the work of Bauer et. al[106], depicts the spectral emissivities of various ceramic materials at different temperatures in the spectral range from 0.8 to 25 μm , the work of Meneses et al. [107], provides the temperature dependent emissivities of Ruby and a rare earth material, Neodymium Gallate($NdGaO_3$).

3. Results and Discussion

A simple Matlab program based on equations 1 to 5, was implemented to quantify the thermal rectification coefficient for different pairs of materials, which takes the emissivity data-set of two different materials and their temperature as input and calculates the forward and reverse bias fluxes, thereby finally giving the value of RTR coefficient as defined in equation 1. Radiative optical properties of the materials under consideration were studied at a temperature difference of 200 K, with $T_1=300\text{K}$ and $T_2=500\text{K}$ while the spectral range taken into account is 1 - 25 μm . This temperature range was considered under the constraints of data availability.

Table.2 shows the list of materials considered in this study, divided into subcategories: metals, semiconductors, ceramics and rare-earth materials for a classified approach. The respective unequal RHF density transmission coefficients in forward and reverse directions for considered pairs of materials are illustrated in Fig.3, while Table 4 summarises the obtained RTR coefficient for all possible pairs of materials with 136 pairs of materials considered in this study.

Among all materials under consideration, Indium Arsenide (InAs) shows the largest values of RTR coefficient, up to 96.35% when used with Ruby($Al_2O_3 : Cr$), as shown in Table.4. The highest value of RTR with materials other than InAs- $Al_2O_3 : Cr$, can invariably be attributed to InAs-TiN which records a value of 95.54%. As can be seen in Table.4, all materials in combination with InAs record more than 50% RTR except Au, which has an

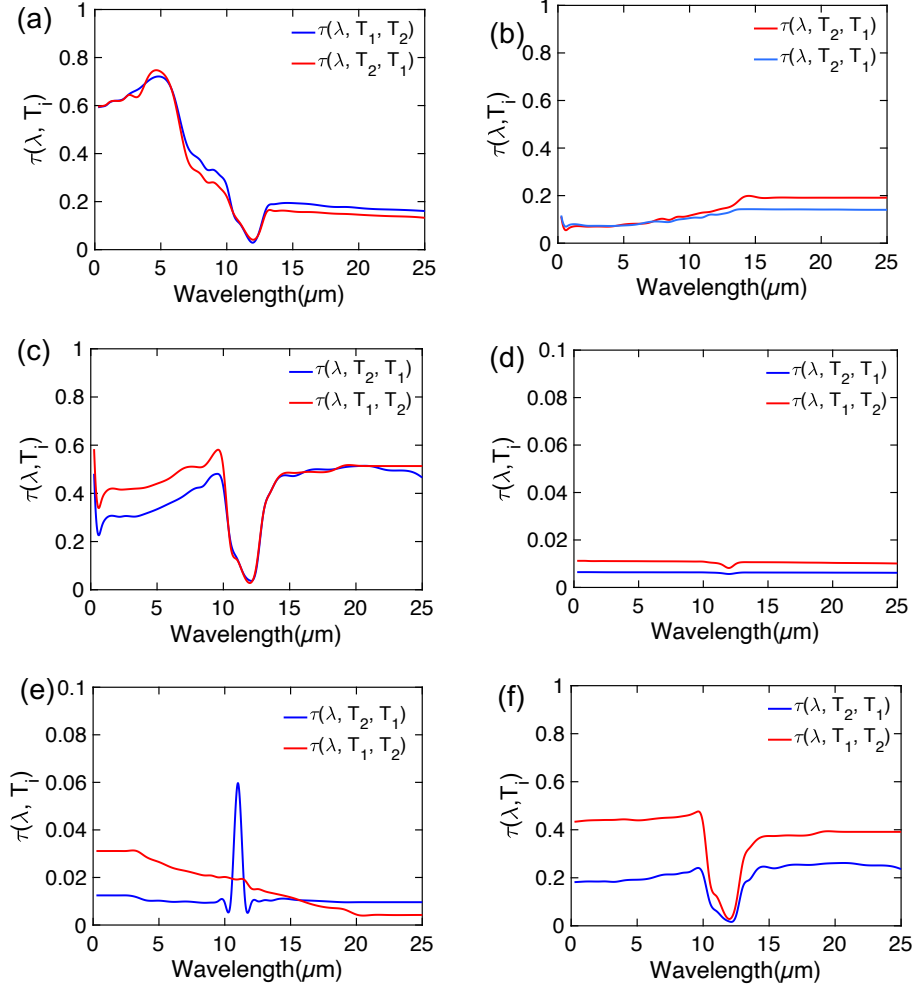


Figure 3: Obtained RHF density transmission coefficients in forward and reverse bias configurations between two materials- (a) SiC/DBuSi($1 \times 10^{20} \text{ cm}^{-3}$) ; (b) GaAs/GaSb; (c) SiC/GaSb; (d) SiC/Au; (e) InAs/Cu (f) InAs/SiC at $T_1=300\text{K}$ and $T_2=500\text{K}$.

RTR value of 45.11%. Au, in fact records greater than 40% with most materials in the table except Ge, GaAs and GaSb. Au-Ge, Au-GaAs combinations yield an RTR coefficient larger than 30% and so does the metal-metal combination of Au-Cu. Among the metals, all material combinations with Ni, consistently record greater than 50% RTR, except with Au, Cu and Al_2O_3 . Most material

Materials	Semiconductors								Metals					Ceramic			Rare Earth
	Ge	GaAs	GaSb	InAs	ZnS	SiC	D Bu Si (3e20)	D Bu Si (1e20)	Au	Cu	Pt	Ni	W	TiN	Al ₂ O ₃	Ruby	NdGaO ₃
Ge	0	1.61	3.71	52.12	17.81	16.00	15.29	16.42	30.11	2.83	7.85	67.11	31.24	37.39	43.67	40.26	36.60
GaAs		0	5.21	51.84	16.42	14.50	13.67	14.95	31.56	4.90	1.26	68.82	8.76	3.94	37.66	4.54	0.54
GaSb			0	47.26	20.67	18.68	17.78	19.22	27.71	0.35	1.63	70.76	8.62	0.023	40.62	0.69	4.35
InAs				0.00	58.80	90.50	58.77	59.37	45.11	59.96	68.38	89.23	94.38	95.54	90.55	96.35	95.49
ZnS					0	1.55	3.49	1.88	43.24	19.27	1.62	69.93	7.58	0.11	39.12	0.40	3.70
SiC						0	1.26	0.36	42.47	20.05	1.54	70.78	9.43	1.4	40.75	2.72	2.94
D Bu Si (3e20)							0	1.43	42.40	19.85	1.64	69.84	7.28	0.40	38.94	0.004	3.92
D Bu Si (1e20)								0	42.41	19.92	1.64	69.83	7.31	0.40	38.92	0.0292	3.93
Au									0	33.63	37.12	28.78	41.98	41.29	39.19	42.44	42.34
Cu										0	12	26.99	18.78	4.79	7.47	20.21	20.12
Pt											0	50.53	2.37	7.53	12.15	1.66	1.33
Ni												0	67.05	63.85	38.88	70.80	69.75
W													0	31.90	33.47	8.43	9.48
TiN														0	20.94	51.13	45.85
Al ₂ O ₃															0	40.64	39.14
Ruby																0	4.87
NdGaO ₃																	0

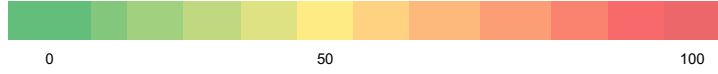


Figure 4: RTR(%) coefficients of thermal rectifiers made of pairs of considered materials for a thermal bias of 200 K.

combinations with Pt yield less than 8% RTR except with InAs and Ni. Among the ceramics, Al₂O₃ combinations with other materials have RTR greater than 20 %, except with Cu and Pt. All other material combinations depicted in Table.4, fall below 30%. The lowest value of RTR is recorded by a combination of D Bu Si(3e20)-(Al₂O₃ : Cr) falling below 0.01%.

In the following paragraphs, we discuss the performances of the different considered materials subcategories, *i.e* semiconductors, metals and ceramic materials with respect to RTR.

Among the semiconductors, InAs exhibits the highest levels of RTR, in combination with most considered materials. This is due to the temperature dependence of its emissivity. As depicted in Fig.2(b), the emissivity increases with increasing temperature and the material becomes more uniformly emissive, contrary to its behaviour at 300 K, where it is more reflective from 1- 5μm,

than other wavelength ranges. Consequently, the radiative heat transfer is lower in this spectral range at low temperatures. Its large emissivity increase when temperature increases directly contributes to material combinations with InAs exhibiting higher RTR. The emissivity of InAs has been shown to strongly depend on its plasmonic properties [115]. On the other hand, it has also been shown that the plasmon energy, *i.e* the plasma frequency, of InAs significantly decreases with increasing temperature[116]. This significant temperature dependence of the plasma frequency in InAs is probably behind the emissivity variation of InAs when temperature increases, hence the large RTR obtained in combination with other materials. For SiC, we observe in Fig.2(e) a slight shift and broadening of the resonance peak of emissivity at around $12\mu\text{m}$ when temperature increases. This is due to anharmonicity effects responsible for the phonon-phonon interactions increase with the temperature [117]. This broadening of the emissivity peak of SiC has certainly an impact on the exchanged radiative heat transfer. However, it is negligible compared to the effect of InAs emissivity temperature dependence when we consider an SiC-InAs based rectifier. For other semi-conductors like Ge, GaSb and GaAs, which do not exhibit a significant emissivity variation as a function of temperature, no marked variation in the radiative heat transfer is observed with these materials when they are considered for RTR.

Among the metals, Ni shows non-negligible RTR of 60% in most material combinations as shown in Table.4. The level of emissivity of Ni as depicted in the work of de Arrieta et al [103], increases with increasing temperature. For most part of the IR wavelengths, Ni remains highly reflective. The curves show the usual behaviour for metallic emissivity, decreasing with wavelength and increasing with temperature. Besides, it can be seen that the temperature dependence is greater in the ferromagnetic phase, ($T < 354^\circ\text{C}$) than in the para-magnetic one. This marked difference in its emissivity behaviours at higher temperatures enables Ni in combination with other materials to yield RTR of 60%. The other metals like Pt[102], Cu [87] and the refractory

metal W [104] exhibit negligible variation of their emissivity as a function of temperature, though showing the same as any metallic emissivity behaviour, elucidating the reason behind such low $RTR(\%) < 5\%$ with most material combinations. This is however not the case for Au[104], where the temperature rise decreases the already low emissivity of the material significantly, making it highly reflective. This is probably why most material combinations with Au have at least $RTR(\%) > 30\%$.

Among the ceramic materials, Al_2O_3 is highly emissive from $6-11\mu m$ and then the emissivity drops to lower levels and also has multiple resonance peaks above $11\mu m$, which broaden as temperatures increase[106]. This behaviour is not observed in either Ruby[107] or TiN[105], where there is almost no difference in emissivity as temperatures increase.

Taking the overall average for each subcategory of materials, the semiconductors fair the best in terms of $RTR(\%)$, closely followed by metals, ceramic materials and rare-earth material. On the other hand, to achieve non-negligible RTR between a pair of materials, at least one of them should exhibit a significant variation of its emissivity as a function of temperature.

Due to constraints of data availability on the materials' thermoradiative properties, a thermal bias $|\Delta T = 200K|$ was chosen which is the most common temperature difference that we found in literature. To enable the generalization of obtained results to other magnitudes of the thermal bias, normalized RTR coefficients were also calculated for all the considered materials.

We show in Table 5, the normalized RTR coefficient which is defined as a ratio of RTR to the magnitude of the considered thermal potential difference $|\Delta T|$. Note that this definition of normalized RTR enables comparison of different pairs of materials operating under different thermal potential differences. However, this particular definition is not applicable for PCM

Materials	Semiconductors								Metals					Ceramic			Rare Earth
	Ge	GaAs	GaSb	InAs	ZnS	SiC	D Bu Si (3e20)	D Bu Si (1e20)	Au	Cu	Pt	Ni	W	TiN	Al ₂ O ₃	Ruby	NdGaO ₃
Ge	0.00	0.01	0.02	0.26	0.09	0.08	0.08	0.08	0.15	0.01	0.04	0.34	0.16	0.19	0.22	0.20	0.18
GaAs		0.00	0.03	0.26	0.08	0.07	0.07	0.07	0.16	0.02	0.01	0.34	0.04	0.02	0.19	0.02	0.00
GaSb			0.00	0.24	0.10	0.09	0.09	0.10	0.14	0.00	0.01	0.35	0.04	0.00	0.20	0.00	0.02
InAs				0.00	0.29	0.45	0.29	0.30	0.23	0.30	0.34	0.45	0.47	0.48	0.45	0.48	0.48
ZnS					0.00	0.01	0.02	0.01	0.22	0.10	0.01	0.35	0.04	0.00	0.20	0.00	0.02
SiC						0.00	0.01	0.00	0.21	0.10	0.01	0.35	0.05	0.01	0.20	0.01	0.01
D Bu Si (3e20)							0.00	0.01	0.21	0.10	0.01	0.35	0.04	0.00	0.19	0.00	0.02
D Bu Si (1e20)								0.00	0.21	0.10	0.01	0.35	0.04	0.00	0.19	0.00	0.02
Au									0.00	0.17	0.19	0.14	0.21	0.21	0.20	0.21	0.21
Cu										0.00	0.06	0.13	0.09	0.02	0.04	0.10	0.10
Pt											0.00	0.25	0.01	0.04	0.06	0.01	0.01
Ni												0.00	0.34	0.32	0.19	0.35	0.35
W													0.00	0.16	0.17	0.04	0.05
TiN														0.00	0.10	0.26	0.23
Al ₂ O ₃															0.00	0.20	0.20
Ruby																0.00	0.02
NdGaO ₃																	0.00

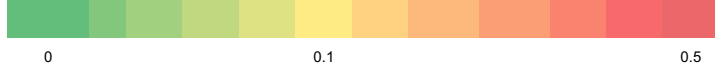


Figure 5: Normalized RTR(%) coefficient i.e RTR coefficients of thermal rectifiers made of pairs of considered materials normalized by the thermal bias.

materials which exhibit a significant change of their radiative properties with a very small temperature variation around their critical temperature which would lead to an infinite normalized RTR.

In Table 6, we present the Temperature Coefficient of total Emissivity (TCE) that can be defined by $\frac{d\epsilon_t}{dT}$, where, ϵ_t is a spectral average with the spectral emissive power as a weighting factor and can be defined as [77]:

$$\epsilon_t = \frac{1}{n^2 \sigma T^4} \int_0^\infty \epsilon_\lambda(T, \lambda) E_{b\lambda}(T, \lambda) d\lambda \quad (6)$$

where, σ is the Stefan–Boltzmann constant, T is the absolute temperature, $\epsilon_\lambda(T, \lambda)$ is the spectral hemispherical emissivity and $E_{b\lambda}(T, \lambda)$ is the blackbody spectral emissive power. This quantity(TCE) has been defined in a similar manner to the refractive index temperature coefficient, $\frac{dn}{dT}$ commonly used in optics[98]. Here due to data availability constraints, a thermal bias of 200 K was considered.

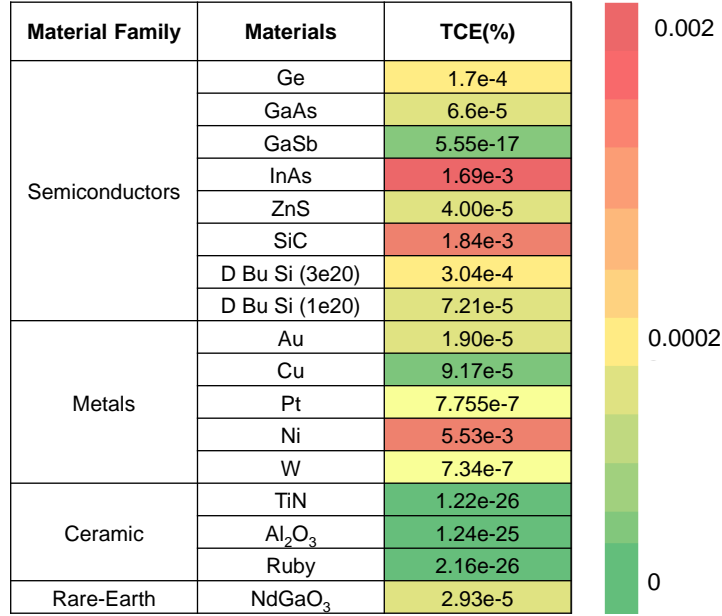


Figure 6: TCE(%) of thermal rectifiers made of pairs of considered materials.

TCE can be used as a key indicator to identify the best candidate materials for thermal rectification since a large variation of radiative properties with respect to temperature is required to obtain a large thermal rectification coefficient. As can be observed in Table 6, the greater the TCE, the more susceptible the materials are for thermal rectification, thus reaffirming the best case of a far field radiative thermal rectifier composed of InAs and SiC.

Results reported in the present manuscript could thus serve as a basic guiding step for researchers and engineers interested in the design of radiative thermal rectifiers for the choice of best candidate materials.

4. Conclusion

We reported in this paper on the thermal rectification potential of 136 pairs of materials commonly used in several applications such as the microelectronics industry. At first, the theoretical concept of thermal

rectification is introduced and the key quantities are defined. Then, used radiative properties, a key parameter for RTR coefficients calculation, are presented. Finally, results of the RTR coefficient of 136 pairs of materials are reported. Obtained results depict that semiconductors show larger RTR coefficient than metals which are in turn better than ceramic materials, due to a non-negligible temperature dependence of the plasmonic properties in such materials which induces a significant emissivity variation as a function of temperature. In particular, InAs-Ruby along with InAs-TiN, InAs-W, InAs-SiC can be very good candidates for a far-field radiative thermal rectifier when combined together with a rectification ratio up to 96.35% for a thermal bias of 200 K. We also show that several pairs of materials provide a relatively high rectification coefficient, larger than 50%. This suggests that they can also be used for thermal rectifiers. A corollary of this result is that non negligible thermal rectification occurs when these pairs of materials are combined in a system with a thermal bias of the order of hundreds of kelvins. Taking into account the temperature dependence of the materials radiative properties is therefore mandatory for an accurate calculation of the exchanged heat flux between these materials in such systems. Presented results may be helpful for thermal management applications and in the advancement of the research and engineering of thermal rectifiers, thermal logical circuits and in thermal energy harvesting.

Acknowledgement

This work was supported by SATT IDF Innov (now Erganeo) in the framework of the project DIOOTHER and by the I-SITE FUTURE Initiative (reference ANR-16-IDEX-0003) in the framework of the project NANO-4-WATER.

References

- [1] C. Starr, The copper oxide rectifier, *Physics* 7 (1) (1936) 15–19.

- [2] J. Miller, W. Jang, C. Dames, Thermal rectification by ballistic phonons in asymmetric nanostructures, in: ASME 2009 Heat Transfer Summer Conference collocated with the InterPACK09 and 3rd Energy Sustainability Conferences, American Society of Mechanical Engineers Digital Collection, 2009, pp. 317–326.
- [3] S. Saha, L. Shi, R. S. Prasher, Monte carlo simulation of phonon backscattering in a nanowire, in: ASME 2006 International Mechanical Engineering Congress and Exposition, American Society of Mechanical Engineers Digital Collection, 2006, pp. 549–553.
- [4] G. Benenti, G. Casati, C. Mejía-Monasterio, M. Peyrard, From thermal rectifiers to thermoelectric devices, in: Thermal Transport in Low Dimensions, Springer, 2016, pp. 365–407.
- [5] B. Sothmann, R. Sánchez, A. N. Jordan, M. Büttiker, Rectification of thermal fluctuations in a chaotic cavity heat engine, *Physical Review B* 85 (20) (2012) 205301.
- [6] A. P. Raman, M. Abou Anoma, L. Zhu, E. Rephaeli, S. Fan, Passive radiative cooling below ambient air temperature under direct sunlight, *Nature* 515 (7528) (2014) 540–544.
- [7] M. A. Kecebas, M. P. Menguc, A. Kosar, K. Sendur, Passive radiative cooling design with broadband optical thin-film filters, *Journal of Quantitative Spectroscopy and Radiative Transfer* 198 (2017) 179–186.
- [8] N. A. Roberts, D. G. Walker, A review of thermal rectification observations and models in solid materials, *International Journal of Thermal Sciences* 50 (5) (2011) 648–662.
- [9] J. Ordonez-Miranda, Y. Ezzahri, J. A. Tiburcio-Moreno, K. Joulain, J. Drevillon, Radiative thermal memristor, *Physical review letters* 123 (2) (2019) 025901.

- [10] P. Ben-Abdallah, S.-A. Biehs, Near-field thermal transistor, *Physical review letters* 112 (4) (2014) 044301.
- [11] K. Joulain, Y. Ezzahri, J. Drevillon, P. Ben-Abdallah, Modulation and amplification of radiative far field heat transfer: Towards a simple radiative thermal transistor, *Applied Physics Letters* 106 (13) (2015) 133505.
- [12] K. Joulain, J. Drevillon, Y. Ezzahri, J. Ordonez-Miranda, Quantum thermal transistor, *Physical review letters* 116 (20) (2016) 200601.
- [13] K. Christoph, M. Reina, R. Messina, P. Ben-Abdallah, B. Svend-Age, Scalable radiative thermal logic gates based on nanoparticle networks, *Scientific Reports* (Nature Publisher Group) 10 (1).
- [14] G. Casati, Device physics: The heat is on—and off, *Nature nanotechnology* 2 (1) (2007) 23.
- [15] S. Murad, I. K. Puri, A thermal logic device based on fluid-solid interfaces, *Applied Physics Letters* 102 (19) (2013) 193109.
- [16] E. Nefzaoui, Y. Ezzahri, K. Joulain, J. Drevillon, Tunable radiative thermal rectifiers: Toward thermal logical circuits, 2015.
- [17] C. Kathmann, M. Reina, R. Messina, P. Ben-Abdallah, S.-A. Biehs, Scalable radiative thermal logic gates based on nanoparticle networks, *Scientific Reports* 10 (1) (2020) 1–11.
- [18] M. J. Martínez-Pérez, A. Fornieri, F. Giazotto, Rectification of electronic heat current by a hybrid thermal diode, *Nature nanotechnology* 10 (4) (2015) 303.
- [19] P. Ben-Abdallah, S.-A. Biehs, Phase-change radiative thermal diode, *Applied Physics Letters* 103 (19) (2013) 191907.

- [20] J. Ordonez-Miranda, K. Joulain, D. De Sousa Meneses, Y. Ezzahri, J. Drevillon, Photonic thermal diode based on superconductors, *Journal of Applied Physics* 122 (9) (2017) 093105.
- [21] A. Ott, R. Messina, P. Ben-Abdallah, S.-A. Biehs, Radiative thermal diode driven by nonreciprocal surface waves, *Applied Physics Letters* 114 (16) (2019) 163105.
- [22] J. Ordonez-Miranda, J. M. Hill, K. Joulain, Y. Ezzahri, J. Drevillon, Conductive thermal diode based on the thermal hysteresis of vo2 and nitinol, *Journal of Applied Physics* 123 (8) (2018) 085102.
- [23] Z. Chen, C. Wong, S. Lubner, S. Yee, J. Miller, W. Jang, C. Hardin, A. Fong, J. E. Garay, C. Dames, A photon thermal diode, *Nature communications* 5 (2014) 5446.
- [24] G. Zhang, H. Zhang, Thermal conduction and rectification in few-layer graphene y junctions, *Nanoscale* 3 (11) (2011) 4604–4607.
- [25] T. Avanesian, G. Hwang, Adsorption-based thermal rectifier, in: *ASME 2015 13th International Conference on Nanochannels, Microchannels, and Minichannels collocated with the ASME 2015 International Technical Conference and Exhibition on Packaging and Integration of Electronic and Photonic Microsystems*, American Society of Mechanical Engineers Digital Collection, 2015.
- [26] A. Reis, I. Smith, Convective thermal rectification in an air-filled parallelogramic cavity, in: *Solar Energy Utilization*, Springer, 1987, pp. 605–617.
- [27] G. Rogers, Heat transfer at the interface of dissimilar metals, *International Journal of Heat and Mass Transfer* 2 (1-2) (1961) 150–154.
- [28] A. Clausing, Heat transfer at the interface of dissimilar metals—the influence of thermal strain, *International Journal of Heat and Mass Transfer* 9 (8) (1966) 791–801.

- [29] D. Lewis, H. Perkins, Heat transfer at the interface of stainless steel and aluminum—the influence of surface conditions on the directional effect, *International Journal of Heat and Mass Transfer* 11 (9) (1968) 1371–1383.
- [30] N. Yang, G. Zhang, B. Li, Carbon nanocone: A promising thermal rectifier, *Applied Physics Letters* 93 (24) (2008) 243111.
- [31] B. Li, L. Wang, G. Casati, Thermal diode: Rectification of heat flux, *Physical review letters* 93 (18) (2004) 184301.
- [32] C. R. Otey, W. T. Lau, S. Fan, Thermal rectification through vacuum, *Physical Review Letters* 104 (15) (2010) 154301.
- [33] M. Francoeur, S. Basu, S. J. Petersen, Electric and magnetic surface polariton mediated near-field radiative heat transfer between metamaterials made of silicon carbide particles, *Optics express* 19 (20) (2011) 18774–18788.
- [34] H. Iizuka, S. Fan, Rectification of evanescent heat transfer between dielectric-coated and uncoated silicon carbide plates, *Journal of Applied Physics* 112 (2) (2012) 024304.
- [35] P. Ben-Abdallah, S.-A. Biehs, Contactless heat flux control with photonic devices, *AIP Advances* 5 (5) (2015) 053502.
- [36] J. Shen, X. Liu, H. He, W. Wu, B. Liu, High-performance noncontact thermal diode via asymmetric nanostructures, *Journal of Quantitative Spectroscopy and Radiative Transfer* 211 (2018) 1–8.
- [37] C. Marucha, J. Mucha, J. Rafałowicz, Heat flow rectification in inhomogeneous gaas, *physica status solidi (a)* 31 (1) (1975) 269–273.
- [38] H. Hoff, Asymmetrical heat conduction in inhomogeneous materials, *Physica A: Statistical Mechanics and its Applications* 131 (2) (1985) 449–464.

- [39] X. Sun, S. Kotake, Y. Suzuki, M. Senoo, Evaluation of thermal rectification at the interface of dissimilar solids by phonon heat transfer, *Heat Transfer—Asian Research: Co-sponsored by the Society of Chemical Engineers of Japan and the Heat Transfer Division of ASME* 30 (2) (2001) 164–173.
- [40] D. B. Go, M. Sen, On the condition for thermal rectification using bulk materials, *Journal of heat transfer* 132 (12).
- [41] J. Hu, X. Ruan, Y. P. Chen, Thermal conductivity and thermal rectification in graphene nanoribbons: a molecular dynamics study, *Nano letters* 9 (7) (2009) 2730–2735.
- [42] X. Yang, J. Xu, S. Wu, D. Yu, B. Cao, The effect of structural asymmetry on thermal rectification in nanostructures, *Journal of Physics: Condensed Matter* 30 (43) (2018) 435305.
- [43] Y. Wang, A. Vallabhaneni, J. Hu, B. Qiu, Y. P. Chen, X. Ruan, Phonon lateral confinement enables thermal rectification in asymmetric single-material nanostructures, *Nano letters* 14 (2) (2014) 592–596.
- [44] J. Lee, V. Varshney, A. K. Roy, J. B. Ferguson, B. L. Farmer, Thermal rectification in three-dimensional asymmetric nanostructure, *Nano letters* 12 (7) (2012) 3491–3496.
- [45] C. W. Chang, D. Okawa, A. Majumdar, A. Zettl, Solid-state thermal rectifier, *Science* 314 (5802) (2006) 1121–1124.
- [46] D. Segal, Single mode heat rectifier: Controlling energy flow between electronic conductors, *Physical review letters* 100 (10) (2008) 105901.
- [47] M. J. Martínez-Pérez, F. Giazotto, Efficient phase-tunable Josephson thermal rectifier, *Applied Physics Letters* 102 (18) (2013) 182602.
- [48] F. Giazotto, F. Bergeret, Thermal rectification of electrons in hybrid normal metal-superconductor nanojunctions, *Applied Physics Letters* 103 (24) (2013) 242602.

- [49] G. T. Landi, E. Novais, M. J. de Oliveira, D. Karevski, Flux rectification in the quantum $x \times x \times z$ chain, *Physical Review E* 90 (4) (2014) 042142.
- [50] R. Scheibner, M. König, D. Reuter, A. D. Wieck, C. Gould, H. Buhmann, L. W. Molenkamp, Quantum dot as thermal rectifier, *New Journal of Physics* 10 (8) (2008) 083016.
- [51] J. Senior, A. Gubaydullin, B. Karimi, J. T. Peltonen, J. Ankerhold, J. P. Pekola, Heat rectification via a superconducting artificial atom, *Communications Physics* 3 (1) (2020) 1–5.
- [52] T. Ruokola, T. Ojanen, A.-P. Jauho, Thermal rectification in nonlinear quantum circuits, *Physical Review B* 79 (14) (2009) 144306.
- [53] L. P. Wang, Z. M. Zhang, Thermal rectification enabled by near-field radiative heat transfer between intrinsic silicon and a dissimilar material, *Nanoscale and Microscale Thermophysical Engineering* 17 (4) (2013) 337–348.
- [54] S. Wen, X. Liu, S. Cheng, Z. Wang, S. Zhang, C. Dang, Ultrahigh thermal rectification based on near-field thermal radiation between dissimilar nanoparticles, *Journal of Quantitative Spectroscopy and Radiative Transfer* 234 (2019) 1–9.
- [55] S. Basu, M. Francoeur, Near-field radiative transfer based thermal rectification using doped silicon, *Applied Physics Letters* 98 (11) (2011) 113106.
- [56] L. Zhu, C. R. Otey, S. Fan, Ultrahigh-contrast and large-bandwidth thermal rectification in near-field electromagnetic thermal transfer between nanoparticles, *Physical Review B* 88 (18) (2013) 184301.
- [57] K. Joulain, Y. Ezzahri, J. Drevillon, B. Rousseau, D. D. S. Meneses, Radiative thermal rectification between SiC and SiO₂, *Optics express* 23 (24) (2015) A1388–A1397.

- [58] G. Xu, J. Sun, H. Mao, T. Pan, Highly efficient near-field thermal rectification between insb and graphene-coated sio₂, *Journal of Quantitative Spectroscopy and Radiative Transfer* 220 (2018) 140–147.
- [59] A. Ghanekar, J. Ji, Y. Zheng, High-rectification near-field thermal diode using phase change periodic nanostructure, *Applied Physics Letters* 109 (12) (2016) 123106.
- [60] Z. Zheng, X. Liu, A. Wang, Y. Xuan, Graphene-assisted near-field radiative thermal rectifier based on phase transition of vanadium dioxide (vo₂), *International Journal of Heat and Mass Transfer* 109 (2017) 63–72.
- [61] A. Fiorino, D. Thompson, L. Zhu, R. Mittapally, S.-A. Biehs, O. Bezenenet, N. El-Bondry, S. Bansropun, P. Ben-Abdallah, E. Meyhofer, et al., A thermal diode based on nanoscale thermal radiation, *ACS nano* 12 (6) (2018) 5774–5779.
- [62] W. Gu, G.-H. Tang, W.-Q. Tao, Thermal switch and thermal rectification enabled by near-field radiative heat transfer between three slabs, *International Journal of Heat and Mass Transfer* 82 (2015) 429–434.
- [63] J. Huang, Q. Li, Z. Zheng, Y. Xuan, Thermal rectification based on thermochromic materials, *International Journal of Heat and Mass Transfer* 67 (2013) 575–580.
- [64] R. St-Gelais, B. Guha, L. Zhu, S. Fan, M. Lipson, Demonstration of strong near-field radiative heat transfer between integrated nanostructures, *Nano letters* 14 (12) (2014) 6971–6975.
- [65] J. Shen, X. Liu, Y. Xuan, Near-field thermal radiation between nanostructures of natural anisotropic material, *Physical Review Applied* 10 (3) (2018) 034029.
- [66] C.-L. Zhou, Y. Zharig, H.-L. Yi, L. Qu, Radiation-based near-field thermal rectification via asymmetric nanostructures of the single material, in:

2019 PhotonIcs & Electromagnetics Research Symposium-Spring (PIERS-Spring), IEEE, 2019, pp. 2652–2658.

- [67] E. Nefzaoui, K. Joulain, J. Drevillon, Y. Ezzahri, Radiative thermal rectification using superconducting materials, *Applied Physics Letters* 104 (10) (2014) 103905.
- [68] E. Nefzaoui, J. Drevillon, Y. Ezzahri, K. Joulain, Simple far-field radiative thermal rectifier using Fabry–Perot cavities based infrared selective emitters, *Applied optics* 53 (16) (2014) 3479–3485.
- [69] R. Audhkhasi, M. L. Povinelli, Design of far-field thermal rectifiers using gold–vanadium dioxide micro-gratings, *Journal of Applied Physics* 126 (6) (2019) 063106.
- [70] K. Ito, K. Nishikawa, H. Iizuka, H. Toshiyoshi, Experimental investigation of radiative thermal rectifier using vanadium dioxide, *Applied Physics Letters* 105 (25) (2014) 253503.
- [71] S. Jia, Y. Fu, Y. Su, Y. Ma, Far-field radiative thermal rectifier based on nanostructures with vanadium dioxide, *Optics letters* 43 (22) (2018) 5619–5622.
- [72] A. Ghanekar, G. Xiao, Y. Zheng, High contrast far-field radiative thermal diode, *Scientific reports* 7 (1) (2017) 1–7.
- [73] H. Prod’homme, Y. Ezzahri, J. Drevillon, K. Joulain, Dynamical behaviour of a far-field radiative thermal transistor, in: 2015 21st International Workshop on Thermal Investigations of ICs and Systems (THERMINIC), IEEE, 2015, pp. 1–4.
- [74] J. Ordonez-Miranda, Y. Ezzahri, J. A. Tiburcio-Moreno, K. Joulain, J. Drevillon, Radiative thermal memristor, *Phys. Rev. Lett.* 123 (2019) 025901. doi:10.1103/PhysRevLett.123.025901.
URL <https://link.aps.org/doi/10.1103/PhysRevLett.123.025901>

- [75] P. Van Zwol, K. Joulain, P. Ben-Abdallah, J. Chevrier, Phonon polaritons enhance near-field thermal transfer across the phase transition of VO₂, *Physical Review B* 84 (16) (2011) 161413.
- [76] D. Sawaki, W. Kobayashi, Y. Moritomo, I. Terasaki, Thermal rectification in bulk materials with asymmetric shape, *Applied Physics Letters* 98 (8) (2011) 081915.
- [77] M. F. Modest, *Radiative heat transfer*, Academic press, 2013.
- [78] S. N. Bose, Planck's law and light quantum hypothesis, *Z. Phys* 26 (1) (1924) 178.
- [79] E. D. Palik, *Handbook of Optical Constants of Solids, Five-Volume Set: Handbook of Thermo-Optic Coefficients of Optical Materials with Applications*, Elsevier, 1997.
- [80] M. J. Weber, *Handbook of optical materials*, Vol. 19, CRC press, 2002.
- [81] A. Beran, The reflectance behaviour of gold at temperatures up to 500° C, *Tschermaks mineralogische und petrographische Mitteilungen* 34 (3-4) (1985) 211–215.
- [82] L. N. Aksyutov, Temperature dependence of the optical constants of tungsten and gold, *Journal of Applied Spectroscopy* 26 (5) (1977) 656–660.
- [83] K. Ujihara, Reflectivity of metals at high temperatures, *Journal of Applied Physics* 43 (5) (1972) 2376–2383.
- [84] J. W. C. De Vries, Temperature and thickness dependence of the resistivity of thin polycrystalline aluminium, cobalt, nickel, palladium, silver and gold films, *Thin Solid Films* 167 (1-2) (1988) 25–32.
- [85] B. Veal, A. Paulikas, Optical properties of molybdenum. i. experiment and kramers-kronig analysis, *Physical Review B* 10 (4) (1974) 1280.

- [86] H. Ehrenreich, H. Philipp, Optical properties of Ag and Cu, *Physical Review* 128 (4) (1962) 1622.
- [87] I. Setién-Fernández, T. Echániz, L. González-Fernández, R. Pérez-Sáez, M. Tello, Spectral emissivity of copper and nickel in the mid-infrared range between 250 and 900 cm⁻¹, *International Journal of Heat and Mass Transfer* 71 (2014) 549–554.
- [88] L. Esaki, Properties of thermally treated germanium, *Physical Review* 89 (5) (1953) 1026.
- [89] T. R. Harris, Optical properties of Si, Ge, GaAs, GaSb, InAs, and InP at elevated temperatures.
- [90] D. Ng, Temperature-dependent reflectivity of silicon carbide.
- [91] K. M. Pitman, A. K. Speck, A. M. Hofmeister, A. B. Corman, Optical properties and applications of silicon carbide in astrophysics, in: *Silicon Carbide-Materials, Processing and Applications in Electronic Devices*, InTech, 2011.
- [92] D. C. Harris, M. Baronowski, L. Henneman, L. V. LaCroix, C. Wilson, S. C. Kurzius, B. Burns, K. Kitagawa, J. Gembarovic, S. M. Goodrich, Thermal, structural, and optical properties of Cleartran® multispectral zinc sulfide, *Optical Engineering* 47 (11) (2008) 114001.
- [93] Y.-B. Chen, Z. Zhang, Heavily doped silicon complex gratings as wavelength-selective absorbing surfaces, *Journal of Physics D: Applied Physics* 41 (9) (2008) 095406.
- [94] S. Basu, L. Wang, Near-field radiative heat transfer between doped silicon nanowire arrays, *Applied Physics Letters* 102 (5) (2013) 053101.
- [95] H. Li, Refractive index of silicon and germanium and its wavelength and temperature derivatives, *Journal of Physical and Chemical Reference Data* 9 (3) (1980) 561–658.

- [96] T. Skauli, P. Kuo, K. Vodopyanov, T. Pinguet, O. Levi, L. Eyres, J. Harris, M. Fejer, B. Gerard, L. Becouarn, et al., Improved dispersion relations for gaas and applications to nonlinear optics, *Journal of Applied Physics* 94 (10) (2003) 6447–6455.
- [97] G. D. Gillen, C. DiRocco, P. Powers, S. Guha, Temperature-dependent refractive index measurements of wafer-shaped inas and insb, *Applied optics* 47 (2) (2008) 164–168.
- [98] M. Bertolotti, V. Bogdanov, A. Ferrari, A. Jascow, N. Nazorova, A. Pikhtin, L. Schirone, Temperature dependence of the refractive index in semiconductors, *JOSA B* 7 (6) (1990) 918–922.
- [99] H. Li, Refractive index of zns, znse, and znte and its wavelength and temperature derivatives, *Journal of physical and chemical reference data* 13 (1) (1984) 103–150.
- [100] D. B. Leviton, B. J. Frey, Temperature-dependent refractive index of cleartran zns to cryogenic temperatures, in: *Cryogenic Optical Systems and Instruments 2013*, Vol. 8863, International Society for Optics and Photonics, 2013, p. 886307.
- [101] G. Hawkins, R. Hunneman, The temperature-dependent spectral properties of filter substrate materials in the far-infrared (6–40 μm), *Infrared physics & technology* 45 (1) (2004) 69–79.
- [102] J. Orosco, C. Coimbra, Temperature-dependent infrared optical and radiative properties of platinum, *International Journal of Heat and Mass Transfer* 143 (2019) 118471.
- [103] I. G. de Arrieta, T. Echániz, J. Olmos, R. Fuente, I. Urcelay-Olabarría, J. Igartua, M. Tello, G. López, Evolution of the infrared emissivity of ni during thermal oxidation until oxide layer opacity, *Infrared Physics & Technology* 97 (2019) 270–276.

- [104] L. Aksyutov, Normal spectral emissivity of gold, platinum, and tungsten, *Journal of engineering physics* 27 (2) (1974) 913–917.
- [105] J. A. Briggs, G. V. Naik, Y. Zhao, T. A. Petach, K. Sahasrabudhe, D. Goldhaber-Gordon, N. A. Melosh, J. A. Dionne, Temperature-dependent optical properties of titanium nitride, *Applied Physics Letters* 110 (10) (2017) 101901.
- [106] W. Bauer, A. Moldenhauer, A. Platzer, Emissivities of ceramic materials for for high temperature processes, in: *Optical Diagnostics*, Vol. 5880, International Society for Optics and Photonics, 2005, p. 58800W.
- [107] D. D. S. Meneses, P. Melin, L. Del Campo, L. Cosson, P. Echegut, Apparatus for measuring the emittance of materials from far infrared to visible wavelengths in extreme conditions of temperature, *Infrared Physics & Technology* 69 (2015) 96–101.
- [108] G. G. Macfarlane, T. P. McLean, J. E. Quarrington, V. Roberts, Fine structure in the absorption-edge spectrum of Ge, *Physical Review* 108 (6) (1957) 1377.
- [109] W. G. Spitzer, D. Kleinman, D. Walsh, Infrared properties of hexagonal silicon carbide, *Physical Review* 113 (1) (1959) 127.
- [110] W. G. Spitzer, D. A. Kleinman, C. J. Frosch, Infrared properties of cubic silicon carbide films, *Physical Review* 113 (1) (1959) 133.
- [111] C. F. Bohren, D. R. Huffman, *Absorption and scattering of light by small particles*, John Wiley & Sons, 2008.
- [112] H. Mutschke, A. C. Andersen, D. Clément, T. Henning, G. Peiter, Infrared properties of SiC particles, arXiv preprint astro-ph/9903031.
- [113] D. Clément, H. Mutschke, R. Klein, T. Henning, New laboratory spectra of isolated -SiC nanoparticles: Comparison with spectra taken by the

Infrared Space Observatory, *The Astrophysical Journal* 594 (1) (2003) 642.

- [114] C. P. Cagran, L. M. Hanssen, M. Noorma, A. V. Gura, S. N. Mekhontsev, Temperature-resolved infrared spectral emissivity of sic and pt-10rh for temperatures up to 900° c, *International Journal of Thermophysics* 28 (2) (2007) 581–597.
- [115] J. Park, J.-H. Kang, X. Liu, S. J. Maddox, K. Tang, P. C. McIntyre, S. R. Bank, M. L. Brongersma, Dynamic thermal emission control with inas-based plasmonic metasurfaces, *Science advances* 4 (12) (2018) eaat3163.
- [116] G. Bell, C. F. McConville, T. Jones, Plasmon excitations and accumulation layers in heavily doped inas (001), *Physical Review B* 54 (4) (1996) 2654.
- [117] L. Sham, J. Ziman, The electron-phonon interaction, in: *Solid State Physics*, Vol. 15, Elsevier, 1963, pp. 221–298.
- [118] P. Herve, L. Vandamme, Empirical temperature dependence of the refractive index of semiconductors, *Journal of Applied Physics* 77 (10) (1995) 5476–5477.

Supplementary Materials I: Radiative properties extraction of considered materials

Table .2: Available data of considered materials

Materials	Reflectivity(ρ)	Transmittivity(t)	Emissivity(ϵ)
Ge	[95]	[89]	$\epsilon=1-\rho-t$
GaAs	[97, 96]	[89]	$\epsilon=1-\rho-t$
GaSb	[118]	[89]	$\epsilon=1-\rho-t$
InAs	[98, 97]	[89]	$\epsilon=1-\rho-t$
ZnS	[92, 99, 100, 101]	[92]	[92]
SiC	$\rho=1-\epsilon$	opaque sample[114]	[114]
Au	[82]	opaque sample[82]	$\epsilon=1-\rho$
Cu	[87]	opaque sample[87]	[87]
Pt	$\rho=1-\epsilon$	opaque sample[102]	[102]
Ni	$\rho=1-\epsilon$	opaque sample[103]	[103]
W	$\rho=1-\epsilon$	opaque sample[104]	[104]
Al_2O_3	$\rho=1-\epsilon$	opaque sample[106]	[106]
$Al_2O_3 : Cr$	$\rho=1-\epsilon$	opaque sample[107]	[107]
TiN	$\rho=1-\epsilon$	opaque sample[105]	[105]
$NdGaO_3$	$\rho=1-\epsilon$	opaque sample[107]	[107]

Radiative optical properties sourced from the works cited in this paper, have provided all the necessary temperature dependent data as is required in this study. Table.2 delineates from which reference the sample radiative optical properties have been gathered and how a particular material property, if not available, of each sample has been calculated. Here, recalling the notations in section 2.1, $\epsilon(\lambda, T)$, $\rho(\lambda, T)$ and $t(\lambda, T)$ are the material emissivity, reflectivity and transmittivity respectively.

Supplementary Materials II: Mapping RTR coefficient of considered materials

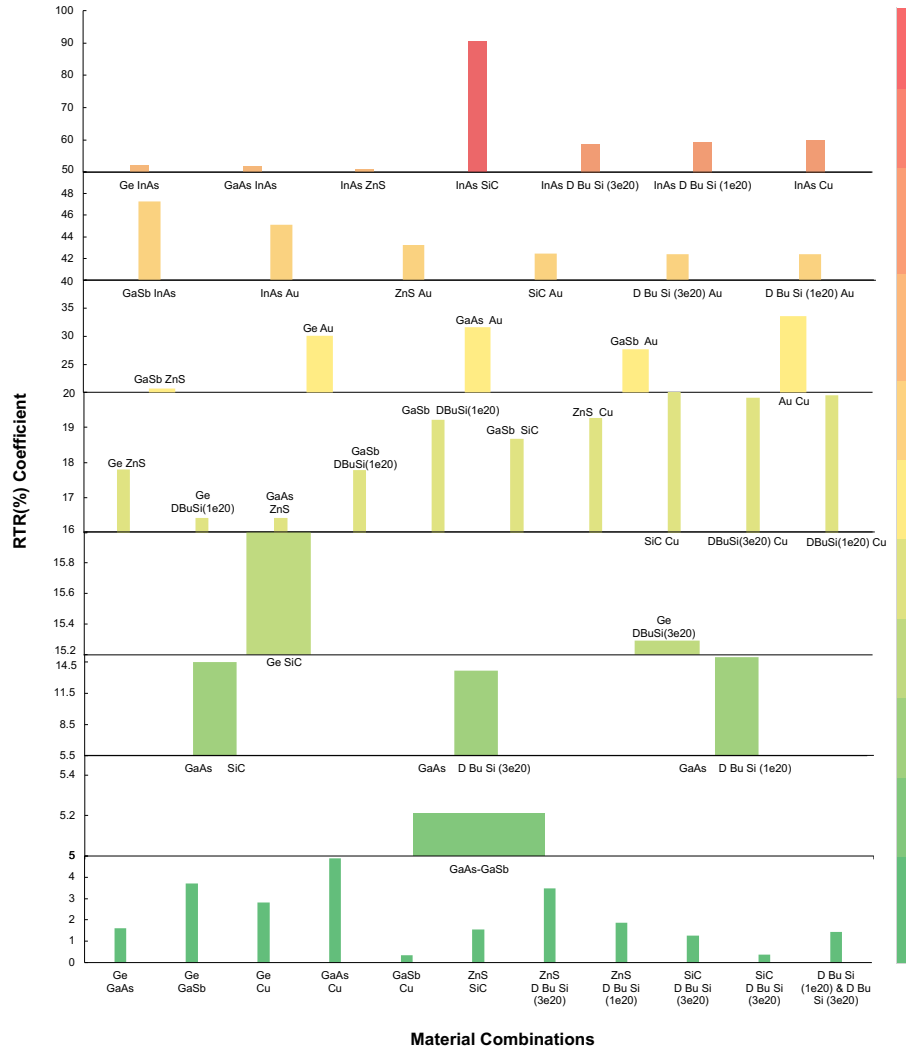


Figure .7: Mapping RTR coefficients of thermal rectifiers made of pairs of considered materials for a thermal bias of 200 K based on the table in Fig.4

As depicted in Table 4, RTR coefficients for different combinations of considered materials, belong to different ranges from 0-91%. In an attempt to streamline and to make each material combination identifiable for an

appropriate RTR coefficient, majority of RTR coefficients are mapped in Figure.7 in different ranges namely: 0-5%, 5-5.5%, 5.5-15.2%, 15.2-16%, 16-20%, 20-40%, 40-50%, 50-100%. These ranges have been ascertained relying on the overall data range in Table 4. Each bar height represents the value of the RTR coefficient and the bar width represents the distribution of entries for each data range. The bar color map corresponds to the amplitude of RTR i.e the lowest values starting from green to red being the highest value obtained. As seen in Figure.7, there are highest no of entries in the range from 16-20% and 0-5%. There are 7 material combinations in the range of 50-100%, which suggests that these combinations have non negligible thermal rectification.